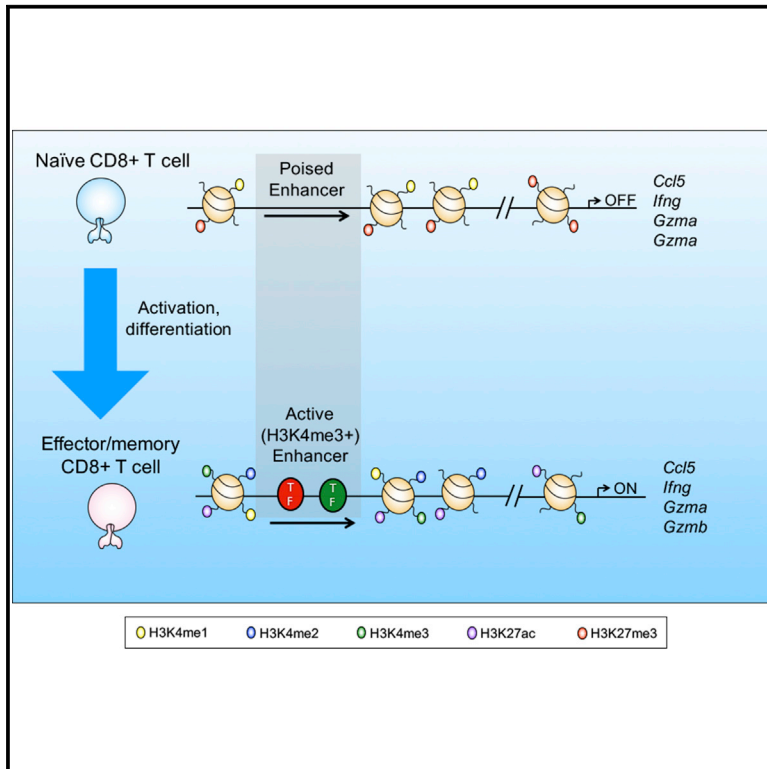


Regulation of H3K4me3 at Transcriptional Enhancers Characterizes Acquisition of Virus-Specific CD8⁺ T Cell-Lineage-Specific Function

Graphical Abstract



Authors

Brendan E. Russ, Moshe Olshansky, Jasmine Li, ..., Paul J. Hertzog, Sudha Rao, Stephen J. Turner

Correspondence

stephen.j.turner@monash.edu.au

In Brief

Russ et al. demonstrate that a subset of poised transcriptional enhancers found in naive virus-specific CD8⁺ T cells acquire a non-canonical chromatin signature upon differentiation. These data provide the genomic location for T cell lineage-specific transcription factor binding that is necessary for virus-specific T cell differentiation.

Highlights

- Virus-specific CTLs exhibit specific changes in enhancer activity upon activation
- H3K4me3 is acquired at lineage-specific enhancers in activated CTL
- H3K4me3 is deposited predominantly at TEs initially poised in the naive state
- H3K4me3⁺ enhancers are specific targets for T cell-specific transcription factors



Regulation of H3K4me3 at Transcriptional Enhancers Characterizes Acquisition of Virus-Specific CD8⁺ T Cell-Lineage-Specific Function

Brendan E. Russ,^{1,2} Moshe Olshansky,^{1,2} Jasmine Li,^{1,2} Michelle L.T. Nguyen,^{2,5} Linden J. Gearing,³ Thi H.O. Nguyen,² Matthew R. Olson,^{1,6} Hayley A. McQuilton,² Simone Nüssing,² Georges Khoury,² Damian F.J. Purcell,² Paul J. Hertzog,³ Sudha Rao,⁴ and Stephen J. Turner^{1,2,7,*}

¹Department of Microbiology, Biomedical Discovery Institute, Monash University, Clayton, VIC 3800, Australia

²Department of Microbiology and Immunology, The Doherty Institute at the University of Melbourne, Parkville, VIC 3010, Australia

³Hudson Institute for Medical Research, Clayton, VIC 3168, Australia

⁴Department of Molecular and Cellular Biology, Canberra University, Canberra, ACT 2000, Australia

⁵Present address: Division of Infectious Diseases, Department of Medicine, University of California, San Francisco, San Francisco, CA 94143, USA

⁶Present address: Department of Pediatrics, Wells Center for Pediatric Research, Indiana University School of Medicine, Indianapolis, IN 46202, USA

⁷Lead Contact

*Correspondence: stephen.j.turner@monash.edu.au

<https://doi.org/10.1016/j.celrep.2017.11.097>

SUMMARY

Infection triggers large-scale changes in the phenotype and function of T cells that are critical for immune clearance, yet the gene regulatory mechanisms that control these changes are largely unknown. Using ChIP-seq for specific histone post-translational modifications (PTMs), we mapped the dynamics of ~25,000 putative CD8⁺ T cell transcriptional enhancers (TEs) differentially utilized during virus-specific T cell differentiation. Interestingly, we identified a subset of dynamically regulated TE that exhibited acquisition of a non-canonical (H3K4me3⁺) chromatin signature upon differentiation. This unique TE subset exhibited characteristics of poised enhancers in the naive CD8⁺ T cell subset and demonstrated enrichment for transcription factor binding motifs known to be important for virus-specific CD8⁺ T cell differentiation. These data provide insights into the establishment and maintenance of the gene transcription profiles that define each stage of virus-specific T cell differentiation.

INTRODUCTION

A cardinal feature of adaptive immunity is the ability of naive B and T cells to acquire, through cellular differentiation, lineage-specific immune functions necessary for pathogen clearance. Upon infection, naive CD8⁺ T cells undergo a proliferative response that coincides with acquisition of effector functions that include the production of anti-viral cytokines (such as interferon-gamma; IFN- γ), cytotoxic molecules (granzymes A and B; GZMA and GZMB) and chemokines (CCL4 and CCL5) (Olson et al., 2010). Importantly, effector differentiation results in the

formation of long-lived, pathogen-specific memory cells, which, relative to their naive precursors, are present at higher frequency and respond more rapidly and robustly to subsequent infections with the same pathogen (Agarwal and Rao, 1998; Veiga-Fernandes et al., 2000). Understanding how cellular differentiation is orchestrated is key to understanding the generation of adaptive immunity. However, many aspects of the molecular basis of cytotoxic T lymphocyte (CTL) differentiation remain to be fully elucidated.

Cellular differentiation is regulated by the strict spatial and temporal control of gene expression, achieved through precise, localized binding of transcription factors (TFs) that activate and repress gene transcription. In turn, the ability of TFs to access the DNA template is modulated by the positioning of histone protein complexes, termed nucleosomes, around which the DNA is wrapped. Nucleosome positioning is regulated by the addition and removal of histone post-translational modifications (PTMs) (Kouzarides, 2007). For instance, acetylation of histone lysine residues reduces nucleosome/DNA interactions, thus increasing genome accessibility and enabling gene transcription (Bauer et al., 1994). Alternatively, methylation at lysine residues can have activating or repressive effects on transcription, depending on the residues methylated and the extent of methylation; trimethylation of histone 3 at lysine 27 (H3K27me3) is associated with nucleosome-dense chromatin and repressed transcription, while di- and trimethylation of H3K4 is associated with less dense nucleosome structures and actively transcribed or transcriptionally poised chromatin (Wang et al., 2008).

Transcriptional enhancers are *cis*-acting DNA regulatory elements occurring within the genome, often many kilobases from their cognate gene promoter, that regulate gene transcriptional activity, in part via the binding of lineage-specific TFs (Spitz and Furlong, 2012). As at gene promoters, the deposition of histone PTMs at transcriptional enhancers (TEs) is tightly controlled in accordance with differentiation state (Visel et al., 2009). Recently, certain enhancers that have been described



as “poised” are characterized by deposition of H3K4me1 and H3K4me2, as well as increased chromatin accessibility, while exhibiting little histone acetylation and enrichment for H3K27me3. These poised enhancers became active, characterized by the loss of H3K27me3 and gain of H3K27Ac, upon initiation of cellular differentiation regulating lineage-specific gene transcription (Orford et al., 2008). It was concluded that this particular enhancer configuration represents a regulatory mechanism enabling rapid transcriptional activation and subsequent cell-lineage commitment of pluripotent cells. What remains to be determined is whether the assessment of such histone PTMs can be used to study TE dynamics beyond stem cell biology and whether this represents a generalized mechanism for control of cell fate decisions in other systems.

While the majority of data on the role played by TEs as regulators of tissue-specific gene expression has come from studies of stem cells, there is mounting evidence that TEs play similar roles in more differentiated cells, including lymphocytes. For instance, a large body of work defines the role of at least 12 separate TEs in controlling IFN- γ transcription in CD4⁺ Th1 cells, CD8⁺ T cells, and natural killer (NK) cells, where they serve as differentiation-dependent binding sites for TFs, including T-bet and STAT4 (Balasubramani et al., 2010; Djuretic et al., 2007; Schoenborn et al., 2007). Surprisingly, given the large number of *Irfng* TEs identified, the deletion of a single TE (–22 kb) markedly reduces IFN- γ production by T cells and NK cells (Balasubramani et al., 2014), implying that the large number of *Irfng* TEs does not reflect functional redundancy and highlighting the importance of TEs as determinants of differentiation-dependent gene expression.

To determine the role of TEs and the TFs with which they interact during the differentiation of virus-specific CD8⁺ T cells, we have mapped the genome-wide deposition of histone PTMs in antigen-specific, naive, effector, and memory CD8⁺ T cells responding to an acute influenza A infection. Here, we define a non-canonical enhancer signature that marks TEs bound specifically by TFs that are linked to T cell lineage-specific gene promoters. These data provide insights into the establishment and maintenance of the gene transcription profiles that define each stage of virus-specific T cell differentiation.

RESULTS

Genome-wide Mapping of H3K4me1/me2 Identifies Putative TEs that Characterize CD8⁺ T Cell Differentiation States

We have previously demonstrated that, upon activation of naive, virus-specific CD8⁺ T cells, large-scale but focused changes in histone methylation patterns (H3K4me3/H3K27me3) occurred at CD8⁺ T cell lineage-specific gene promoters (Russ et al., 2014). Importantly, the particular dynamics of histone PTM loss and gain at promoters identified functionally distinct classes of genes and provided a basis for the coordinated regulation of CTL differentiation (Russ et al., 2014). Given that this initial study only focused on gene promoters, we sought to further expand this analysis by determining the dynamics of TE usage during CD8⁺ T cell differentiation. To this end, naive (CD44^{lo}, CD62L^{hi}) OT-I TCR transgenic CD8⁺ T cells (specific for the ovalbumin peptide OVA_{257–264}), were adoptively transferred into congenic

C57BL/6J (B6) hosts, followed by infection intranasally (i.n.) with the influenza A/HKx31-OVA virus (Jenkins et al., 2006). We have previously shown that ovalbumin peptide (257–264, (OT-I))-specific CTLs respond in a numerically and functionally equivalent way to a normal endogenous influenza CD8⁺ T cell response (Jenkins et al., 2006, 2007). Chromatin immunoprecipitation sequencing (ChIP-seq) for the H3K4me1 modification was performed on sort-purified (>99% purity) naive (day 0), effector (day 10), and memory (>60) OT-I T cells and combined with H3K4me2 data obtained previously (Russ et al., 2014). During pluripotent cell differentiation, acquisition of H3K4me2, as well as its co-localization with H3K4me1, has been used to define TEs that have the potential to be either poised or active (Orford et al., 2008; Zhang et al., 2012). As such, this definition allowed us to generate a preliminary analysis of the dynamics of *de novo* TE activity across the distinct phases of T cell differentiation in response to virus infection. We first identified potential TEs for each stage of differentiation (defined as H3K4me1⁺ H3K4me2⁺; Experimental Procedures). A total of ~25,000 peaks were identified with the majority of those located between 5 and 500 kb distant to the transcriptional start site of associated genes (Figure 1A). While each differentiation state was characterized by a unique set of H3K4me1⁺me2⁺ TEs, many (~45%) were shared by all states (Figure 1B). This signature enabled the identification of known TEs, such as those associated with the *Irfng* (Balasubramani et al., 2010; Schoenborn et al., 2007) (Figure 1C) and *Il2ra* loci; Figure S2). Further, this same signature could be used to identify putative TEs associated with lineage-specific CD8⁺ T cell genes, including TEs associated with *Gzmb* (which encodes the prototypic cytolytic molecule, granzyme B; Figure 1D), *Gzma* (Figure 1E), and *Gzmk* (Figure 1F).

To further assess the nature of TEs that undergo H3K4me1/me2 modulation, we identified potential TEs that were dynamically regulated upon naive CD8⁺ T cell differentiation into effector/memory (E/M) T cells. There were approximately 3,500 and 3,600 me1/me2 regions that were uniquely present in virus-specific E/M or naive OT-I CD8⁺ T cells, respectively (Table S1). The acquisition of me1/me2 upon differentiation often occurred at genomic elements that were embedded within a cluster of TEs already marked with me1/me2 in the naive state (e.g., –6-kb *Irfng* TE [Figure 1C]; and +18-Kb *Il2ra* TE [Figure S2]). We also identified TEs that exhibited loss of me1/me2 domains upon naive CD8⁺ T cell differentiation into E/M CTLs that were associated with an overall transcriptional downregulation of associated genes, and interestingly, genes regulated in this way were also predominantly immune genes (Figure S1). For instance, this included several naive T cell-specific chemokine receptors such as *Ccr7*, *Ccr4*, and *Ccr9* and TFs such as *Sox13*—an important regulator of the Wnt/ β -catenin signaling pathway (Figure S1).

We utilized GREAT for Gene Ontology (GO) analysis (McLean et al., 2010) to gain a further understanding of the biological function of genes associated with the TEs uniquely observed in either the E/M or the naive T cell states (Figures 1G and S1B). TEs acquired by effector and memory OT-I T cells were associated with genes that were enriched with both broad and T cell-specific immunological function (Figure 1G; Table S2). This included known regulators of T cell differentiation (*Gata3*, *Id2*, *Irf4*, *Prmd1*, *Stat3*, *Stat4*, and *Stat5a*), cytokine and chemokine

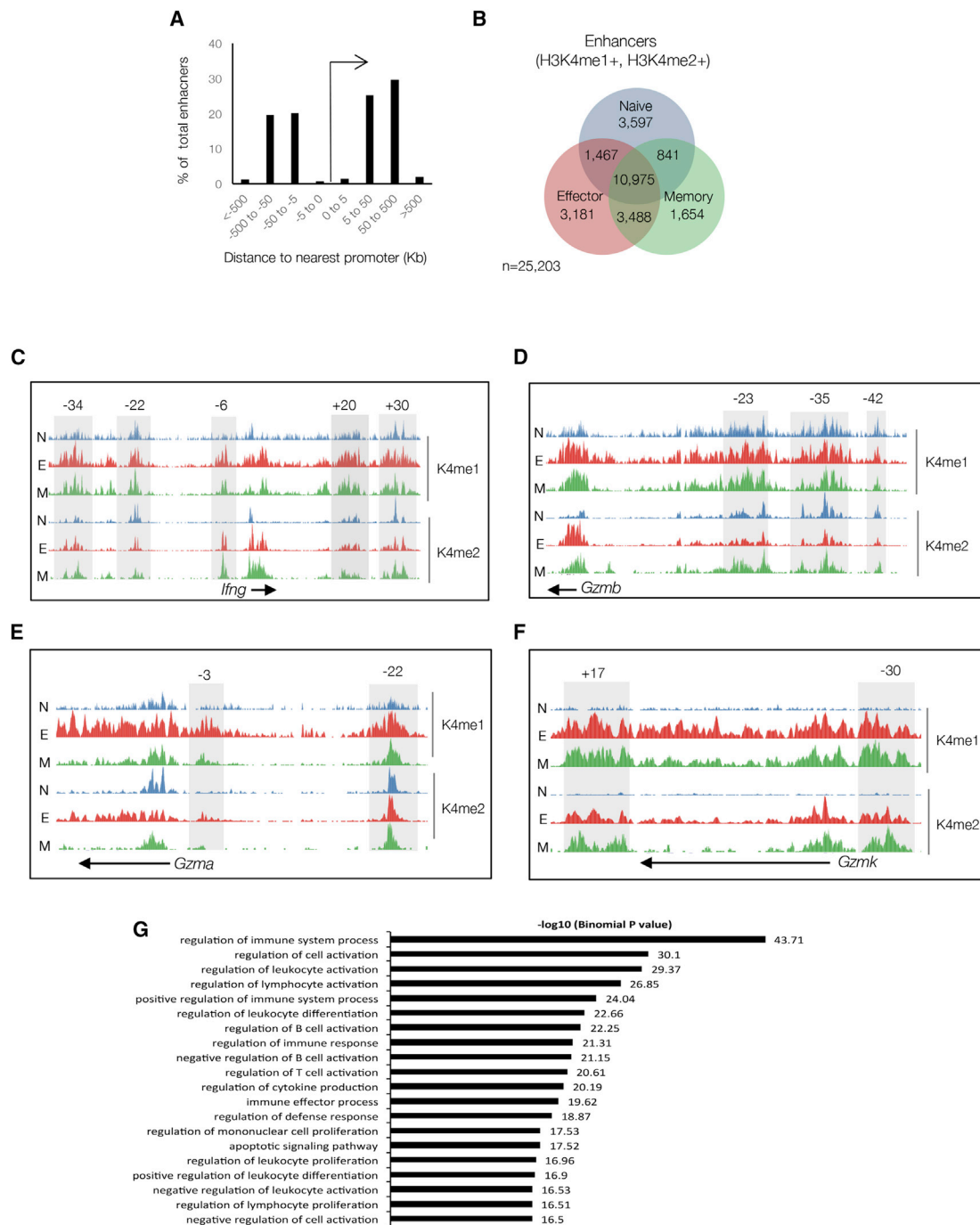


Figure 1. Putative H3K4me1/H3K4me2 Enhancer Dynamics during Virus-Specific CTL Differentiation

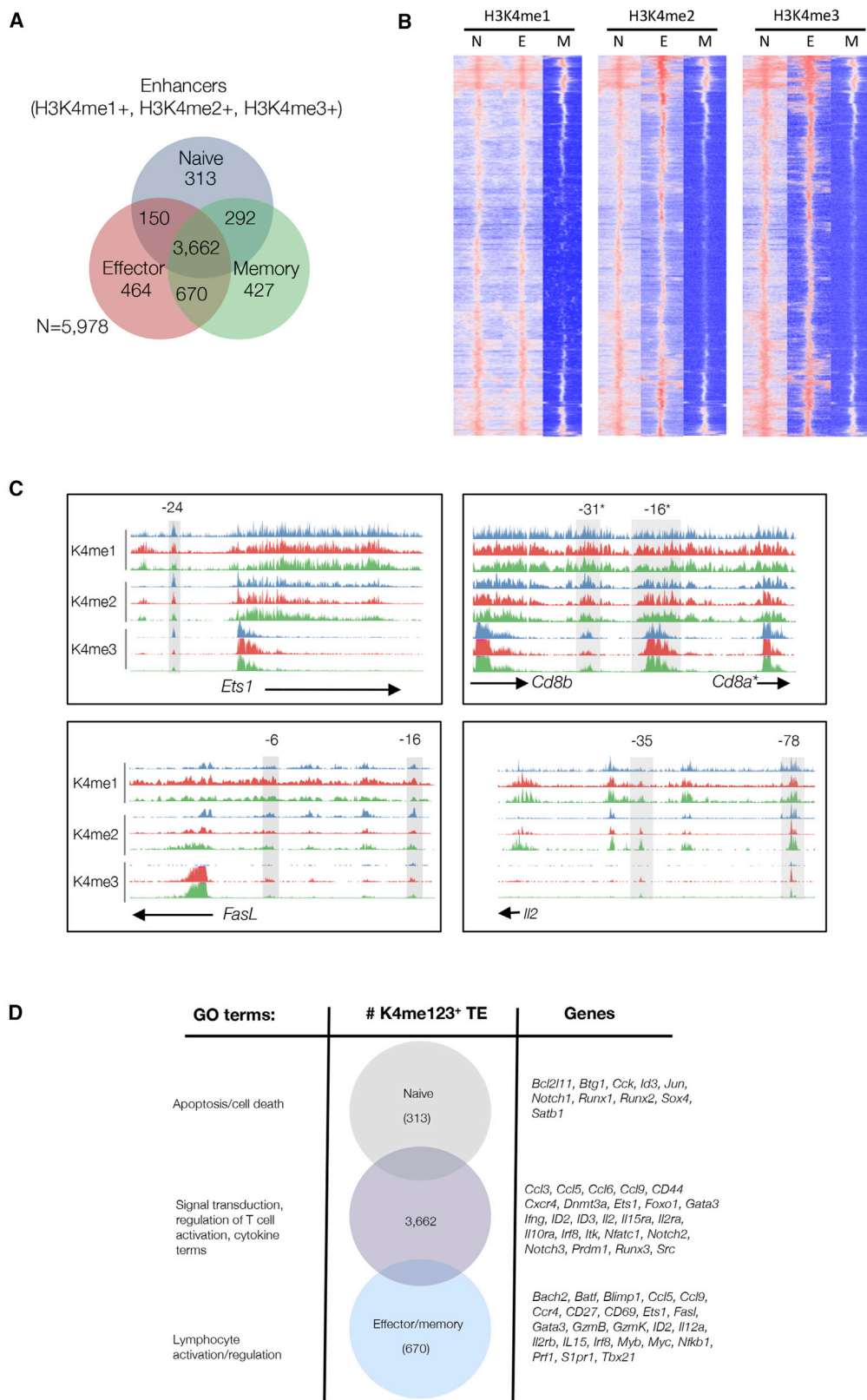
Naive ($CD44^{\text{lo}}CD62L^{\text{hi}}$) $CD45.1^+ CD8^+$ OT-I CTLs were sort purified prior to adoptive transfer into $CD45.2^+$ congenic mice. Mice that had received naive OT-I were infected with A/HKx31-OVA and effector ($CD44^{\text{hi}}CD62L^{\text{lo}}$), and memory ($CD44^{\text{hi}}$) OT-I were isolated and sort purified either 10 or 60 days after infection, respectively. ChIP-seq using an Illumina HiSeq 2500 was performed on naive, effector, and memory $CD8^+$ OT-I T cells for H3K4me1, with data mapped onto the mouse genome (version mm10), and overlapping peaks for H3K4me1 and H3K4me2 (Russ et al., 2014) that were called for naive, effector, and memory OT-I.

(A) Shown is the genomic location to the nearest TSS of putative H3K4me1 $^+$ H3K4me2 $^+$ peaks.

(B) Shown is the number and overlap of H3K4me1 $^+$ /H3K4me2 $^+$ peaks identified for naive, effector, and memory OT-I $^+$ T cells.

(C–F) Shown are tracks for H3K4me1 and H3K4me2 peaks for CTL effector gene loci for naive (blue), effector (red), and memory (green) OT-I. (C) *Ifng*, (D) *Gzmb*, (E) *Gzma*, and (F) *Gzmk*. Both known and putative TEs are highlighted with gray boxes.

(G) GREAT was utilized for Gene Ontology analysis of genes linked to *cis*-regulatory elements that demonstrated a gain of H3K4me1 $^+$ /me2 $^+$ peaks upon naive OT-I differentiation into the E/M state.



(legend on next page)

genes (*Ccl3*, *Ifng*, *Il2*, *Il6*, *Il15*, *Il21*, and *Il27*), and cytokine and chemokine receptors (*Ccr2*, *Ccr3*, *Ccr5*, *Cxcr1*, *Cxcr3*, *Cxcr4*, *Ifngr1*, *Il12ra*, *Il2ra*, *IL20ra*, and *Il23r*). Interestingly, putative TEs within naive T cells that lost me1/me2 upon differentiation included genes associated with negative regulation of metabolic processes and DNA transcription/translation (Figure S1B; Table S2). This supports the concept that naive T cell activation is associated with a rapid switch in the metabolic profile that is required to sustain cellular proliferation (Pearce et al., 2013). Interestingly, there was also a loss of TEs linked to genes associated with immunological function (Figure S1B; Table S2). This included genes known to be associated with the Wnt/ β -catenin signaling pathway (*Lef1*, *Ccr7*, *Runx1*, *Runx2*, and *Satb1*), a process important for maintaining naive CD8⁺ T cell identity (Muralidharan et al., 2011). These data suggest that, in addition to the activation of TEs that likely drive acquisition of CTL-lineage-specific function, there is a need to inactivate specific TEs that enforce active maintenance of a naive T cell state.

It was, then, of interest to determine whether these same TEs exhibited characteristics of poised TEs (Orford et al., 2008). We examined the histone signatures of gene loci upregulated upon naive CD8⁺ T cell activation to determine whether they were, in fact, poised TEs (K4me1⁺/K4me2⁺/K27me3⁺) in the naive state and became active (K4me1⁺/K4me2⁺/K27me3⁻/K27Ac⁺) upon differentiation. Of the 765 genomic regions that were H3K4me1/2⁺ in the naive state, 589 (~75%) were poised (H3K27me3⁺), becoming active (H3K27Ac⁺) upon E/M differentiation. Examples of poised enhancers included those associated with *Tbx21*, *Prdm1*, *Irf8*, *Fasl*, *Il2ra*, and *Klrg1* (Figure S2A). Indeed, Gene Ontology analysis demonstrated that genes associated with “poised” TEs were enriched for immunological terms (Figure S2B). Taken together with the initial observations stated earlier, these data suggest that virus-specific T cell differentiation is underpinned by a combination of *de novo* TE gain and loss with a subset of “poised” TEs present within naive T cells.

H3K4me3 Marks a Subset of Active TEs

While H3K4me3 deposition is typically associated with active gene promoters, in some instances it has been reported to have been associated with enhancers (Pekowska et al., 2011). We have previously shown that ~30% of peaks of H3K4me3 enrichment within virus-specific CD8⁺ T cells map to intergenic regions (Russ et al., 2014). Together, these findings implicate this signature as identifying a unique subset of TEs (Barski et al., 2007; Wang et al., 2008) in T cells. Indeed, 5,978 (~25%) of the H3K4me1⁺/H3K4me2⁺ TEs overlapped intergenic H3K4me3 peaks (Figures 2A and 2B). Just over half (~53%) of the TEs defined by H3K4me1, H3K4me2, and H3K4me3⁺ (me3⁺) TEs were shared between naive, effector, and memory differentiation states (e.g., *Ets1* and *Cd8a*; Figure 2C, top).

K4me3 was acquired at a subset of the regulated TEs (Figure 2A; Table S3) upon naive CD8⁺ T cell differentiation into effector and memory states (e.g., *Fasl* and *Il2*; Figure 2C, bottom; Tables S2 and S3). Importantly, all of these H3K4me3⁺ TEs were also H3K27Ac⁺, indicative of being active TEs (Figures S3A and S3B; e.g., *Ifng* –6-kb TE). In line with this, the deposition of H3K4me3 at active enhancers in effector and memory CTLs was also broadly associated with increased levels of transcription of associated genes (Figure S3C).

H3K4me1⁺/me2⁺/me3⁺ TEs that are present only within naive CD8⁺ cells showed enrichment for GO terms relating to the regulation and maintenance of pluripotency (e.g., “stem cell maintenance,” “somatic stem cell maintenance,” and “regulation of stem cell differentiation”); Figure 2D), consistent with their increased differentiation potential relative to effector and memory states. While H3K4me3⁺ TEs shared by all three differentiation states were largely enriched for T cell and lymphocyte-related terms (e.g., “T cell activation” and “regulation of T cell activation”), terms relating to general cellular functions were also enriched (e.g., “positive regulation of mRNA catabolic processes,” “protein binding,” and “negative regulation of transferase activity”). GO analysis of genes associated with me3⁺ TEs only found in E/M CTLs showed enrichment for immune-related genes that included both key CD8⁺ T cell TFs (*Gata3*, *Prdm1*, and *Tbx21*) and effector gene loci (*Ccl5*, *Ifng*, *Gzma*, *Gzmb*, *Gzmk*, and *Prf1*; Figure 2D).

H3K4me3⁺ Enhancers Bind TFs that Control T Cell Differentiation

The analyses described earlier suggested that H3K4me3 marks a subset of TEs that specifically drive transcription of differentiation-dependent T cell-specific immune genes. Based on this observation, we hypothesized that me3⁺ enhancers acquired upon CTL differentiation would contain TF binding sites (TFBSs) known to be essential for T cell differentiation. Utilizing a TFBS enrichment algorithm termed CiiDER (Supplemental Information), we identified the enrichment of known TF motifs within me3⁺ TEs shared by effector and memory cells against a background of total me1⁺me2⁺me3⁺ TEs, reasoning that the former group would contain TFBSs that specifically drive E/M CTL differentiation (Figure 3A). Consistent with our hypothesis, motifs for known regulators of effector and memory T cell differentiation, including BATF/JUN (AP1), T-BET, EOMES, BCL6, BLIMP1, and GATA3, were specifically enriched within me123⁺ TEs of E/M T cells (Figure 3A). Moreover, we observed that particular motifs, including those of ONECUT3 and POU family members, also demonstrated significant enrichment and may be indicative of a previously unrecognized role for these TFs in the regulation of CTL differentiation. It was also of interest to observe that there was decreased enrichment for particular TFBSs within me3⁺ TEs upon naive CD8⁺ T cell differentiation into E/M CTLs (Figure 3A).

Figure 2. Identification and Characterization of H3K4me3⁺ TEs within Naive, Effector, and Memory IAV-Specific CTLs

- (A) Shown is the number of H3K4me1⁺/H3K4me2⁺ TEs that exhibited H3K4me3 peaks in naive, effector, and memory OT-1 CD8⁺ T cells.
 (B) Heatmaps showing the distribution of H3K4me1, H3K4me2, and H3K4me3 at TEs within naive (N), effector (E), and memory (M) OT-1 CD8⁺ T cells.
 (C) H3K4me1/me2/me3 ChIP-seq tracks for selected gene loci in naive (blue), effector (red), and memory (green) CD8⁺ OT-1 T cells, with H3K4me3⁺ TEs highlighted in gray.
 (D) Gene Ontology analysis showed that H3K4me3⁺ TEs are enriched at genes encoding TFs and effector molecules.

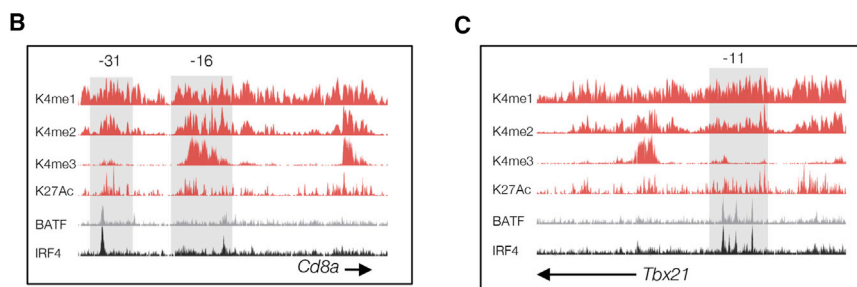
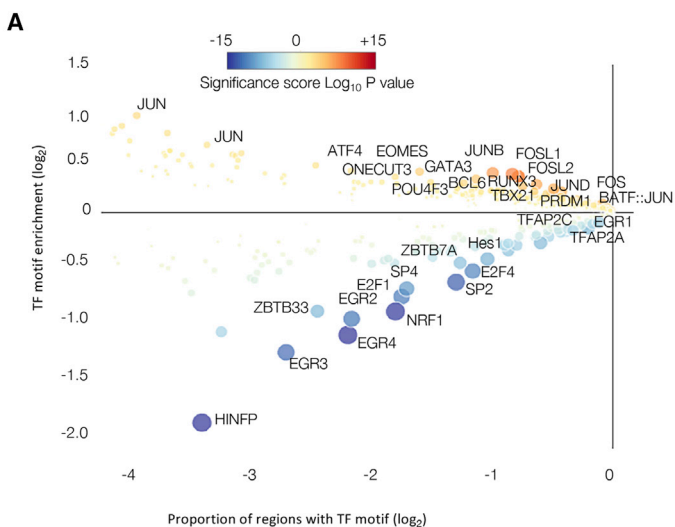


Figure 3. Enrichment of T Cell-Lineage TFBSs within H3K4me3⁺ TEs Uniquely Acquired upon IAV-Specific Effector/Memory CD8⁺ T Cell Differentiation

(A) TFBS enrichment analysis, using CiiIDER (L.J. Gearing and P.J. Hertzog, unpublished data), of H3K4me3⁺ TEs shown to be unique to IAV-specific effector and memory CD8⁺ OT-I. Shown is the proportion (log₂) of H3K4me3⁺ TEs that exhibited specific enrichment of TFBS (x axis), the degree of enrichment (log₂), and either gain of sites (red/yellow) or loss of sites (blue), with the size of the circle indicative of the significance score.

(B and C) Effector OT-I (d10) ChIP-seq tracks for H3K4me1, H3K4me2, H3K4me3, and K27Ac overlaid with data for IRF4 and BATF binding (Kurachi et al., 2014). Also indicated is the binding of IRF4 and BATF at genomic locations that overlap with H4K4me3⁺ TEs in effector OT-I (gray box).

(B) *Cd8a*.

(C) *Tbx21*.

This included loss of motif enrichment for TFs known to regulate T cell thymic maturation and maintenance of the naive T cell state, including *Egr1*, *Egr2*, *Egr3*, and *Zbtb7a* (Figure 3A). To determine whether the motifs enriched within E/M states were bound by the predicated TFs, we overlaid published ChIP-seq data for IRF4 and BATF (Kurachi et al., 2014) onto our ChIP-seq analyses. Despite the fact that the TF data were derived from *in-vitro*-stimulated T cell cultures, there was clearly an overlap of BATF/IRF4 binding at me3⁺ enhancers unique to E/M states (Figure 3B). Importantly, there was greater overlap of BATF/IRF4 binding and H3K4me3⁺ peaks within the E/M state when compared to the naive state. 175 (~16%) of the 1,069 unique E/M H3K4me3⁺ TEs bound BATF/IRF4 versus 10 (~1.6%) of the 617 unique naive H3K4me3⁺ TEs (data not shown). Hence, H3K4me3⁺ marks TEs associated with immune-related gene loci that are targets for key TFs known to drive CTL differentiation.

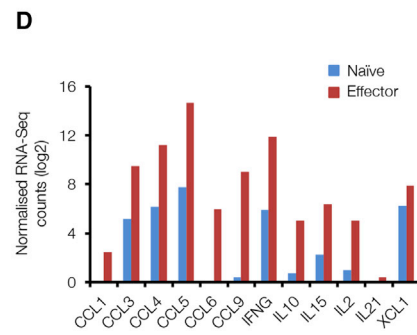
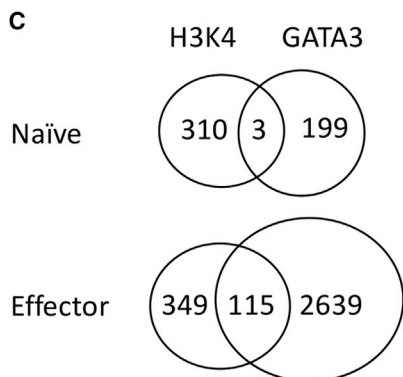
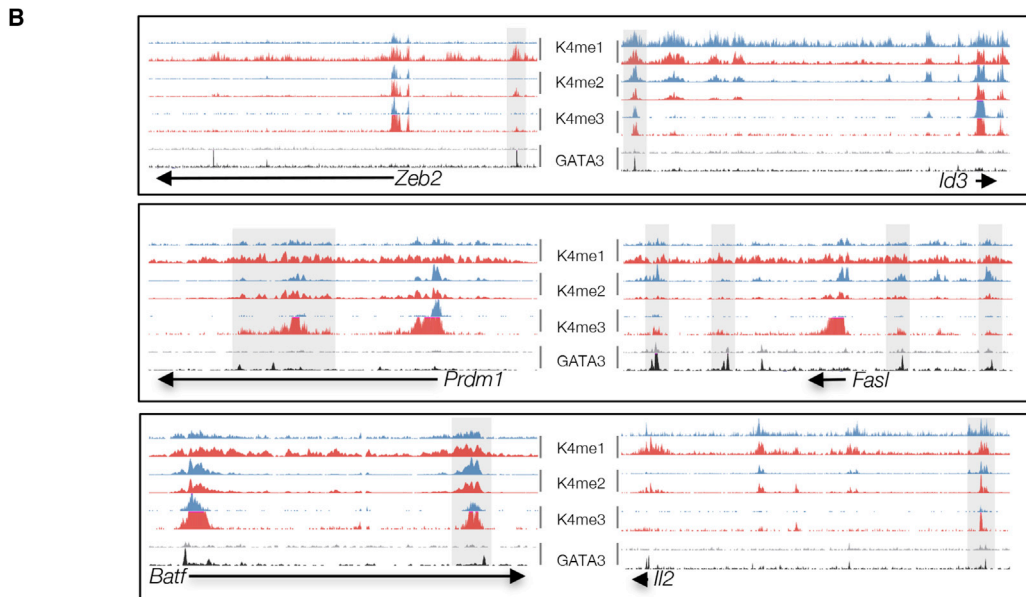
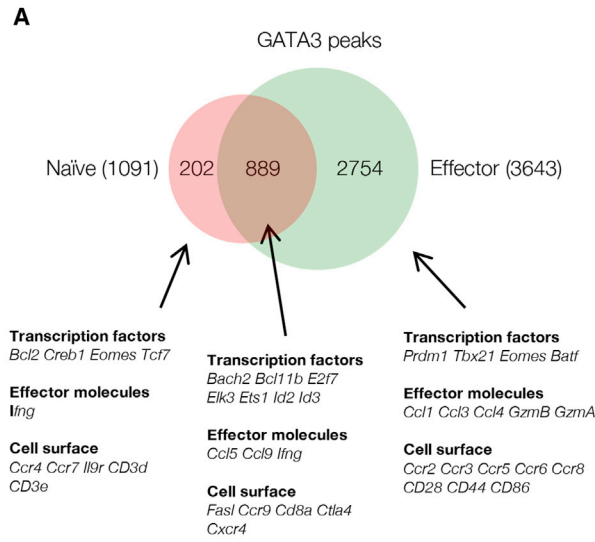
Unique Effector/Memory H3K4me3⁺ TEs Are Targets for GATA3 Binding

While GATA3 is primarily associated with CD4⁺ T_H2 T cell differentiation (Zhu et al., 2010), GATA3-deficient CD8⁺ T cells are unable to generate mature effector CTL responses (Wang et al., 2013). Despite the implication that GATA3 is, therefore, a key regulator of CTL differentiation, there is little known about the genomic targets or proposed mechanisms of action

of GATA3 within virus-specific CTLs. Given that GATA3 motifs were strongly enriched within E/M me3⁺ TEs (Figure 3A), GATA3 ChIP-seq was carried out on naive and virus-specific effector T cells to determine whether these motifs were bound by GATA3. We mapped 202 GATA3 binding sites unique to naive T cells, and 2,754 sites unique to effector T cells, with 889 sites common to both

states (Figure 4A). We have previously demonstrated that GATA3 binds to the *Gzma* locus within effector CTLs (Nguyen et al., 2016). Analysis of the GATA3 ChIP-seq data confirmed that GATA3 was bound to the *Gzma* locus at the me3⁺ TE within influenza (IAV)-specific effector, but not naive, CD8⁺ T cells (Figure S4A). Interestingly, we observed a similar pattern for me3⁺ putative TEs linked to the *Gzmb* locus (Figure S4B).

The aforementioned data suggested that GATA3 may, in fact, be bound to TEs linked to signature CTL gene loci within effector, but not naive, CD8⁺ T cells. There were clear differences between the types of genes bound by GATA3 within naive and effector cells; within naive cells, GATA3 bound genes associated with maintenance of cell pluripotency and regulation of apoptosis but, notably, few genes associated with CTL effector function, or key T cell TFs (Table S4). By contrast, within effector CTLs, there was a strong preference for GATA3 binding at effector genes (e.g., *Il2*, *Fasl*, *Ccl4*, *Ccl5*, and *Il15*, Figure 4B; Table S4), and at TFs that orchestrate effector and memory T cell differentiation (e.g., *Batf*, *Zeb2*, *Prdm1*, *Id3*, *Tbx21*, and *Irf4*; Figure 4B; Table S4). Strikingly, of the 313 me3⁺ TEs uniquely observed in naive CTLs, only 3 (~1.0%) were bound by GATA3 (Figure 4C). In contrast, of the 464 me3⁺ TEs found only within effector CTLs, 115 (~25%) were bound by GATA3 (Figure 4C). Finally, the binding of GATA3 to me3⁺ enhancers was associated with increased signature T cell effector gene transcription within effector CTLs (Figure 4D), suggesting that



(legend on next page)

GATA3 binding is targeted to TEs that acquire me3⁺ upon effector differentiation and associated with transcriptional activation of effector-specific genes.

Induction of *Ccl5* Transcription Correlates with GATA3 Binding and Changes in Chromatin Composition

We identified GATA3 TFBSs within two putative TEs –4 kb and –20 kb upstream of the CTL effector gene, *Ccl5* (Figure 5A). Importantly, both of these TEs demonstrated H3K4me3-specific deposition in E/M CTLs, which was not present within naive CD8⁺ OT-I T cells (Figure 5A). GATA3 was bound to the *Ccl5* –20-kb enhancer within effector, but not naive, IAV-specific CD8⁺ T cells, and this was associated with an active K4me3⁺ TE signature, increased *Ccl5* transcription, and CCL5 protein expression (Figures 5A–5D).

To determine whether the differences in *Ccl5* gene expression observed for the various activation states could be explained by regulation of the chromatin state across the *Ccl5* locus, we performed formaldehyde-assisted isolation of regulatory elements (FAIRE) (Giresi et al., 2007) and ChIP assays to measure chromatin accessibility and the deposition of selected histone PTMs, within *in-vitro*-activated naive and effector CTLs using primers spanning a region from ~250 bp upstream of the *Ccl5* promoter to just beyond the –20-kb TE (Figure 5E). This region encompassed the TEs defined as H3K4me1⁺/me2⁺/me3⁺ by our ChIP-seq analysis (Figure 5A), with the region in between serving as a negative control, given that changes in the chromatin profile and accessibility were not expected.

In line with our preliminary ChIP-seq data (Figure 5A), both the –4- and –20-kb TEs exhibited a poised state, with both elements demonstrating accessible chromatin, as well as enrichment for both H3K4me2 and H3K27me3, and lacking H3K27Ac (Figure 5E, blue line). Upon T cell activation, both putative *Ccl5* TEs acquired an active epigenetic signature with greater chromatin accessibility, loss of H3K27me3, and gain of H3K27Ac (Figure 5E, green line). It was interesting to note that the –4-kb *Ccl5* TE already demonstrated a strong H3K4me2 signature in the naive state, with no increase in H3K4me2 enrichment upon activation. This contrasted with the –20-kb enhancer that did show increased H3K4me2 enrichment upon activation (Figure 5E). Strikingly, when compared to naive CD8⁺ T cells, there was clear enrichment of H3K4me3 at both the *Ccl5* –4- and –20-kb TEs upon T cell activation, suggesting that establishment of H3K4me3 at active TEs is associated with the acquisition of differentiation-dependent CTL effector function.

To test whether the –20-kb TE described earlier physically interacts with the *Ccl5* promoter, we performed chromatin

conformation capture (3C) assays, using a probe located within the 5' UTR of the *Ccl5* gene (Figure S5). The 3C technique did not have sufficient resolution to provide a reliable measure to discriminate specific interactions between the *Ccl5* promoter and –4-kb enhancer. Analysis of the *Ccl5* promoter and *Ccl5* –20-kb TE interactions demonstrated a clear peak of interaction in effector CD8⁺ T cells (Figure S5, blue line). Thus, transcriptional activation of *Ccl5* upon naive CD8⁺ T cell activation is associated with close physical contact between the *Ccl5* –20-kb TE and *Ccl5* gene promoter. Given that CCL5 expression is linked to activated CD8⁺ T cell differentiation, it was surprising to observe that the *Ccl5* –20-kb TE was already in close contact with the promoter in naive CD8⁺ cells, in a manner similar to that of activated effector CTLs (Figure S5, green line). This suggests that the *Ccl5* locus within naive CD8⁺ T cells is already configured in a way to enable rapid *Ccl5* transcription.

We then extended the *Ccl5* 3C analysis to probe potential interactions between the *Ccl5* promoter and regions that covered approximately 140 kb upstream and included the *Ccl9*, *Ccl3*, and *Ccl4* gene loci. While no interactions were detected with the *Ccl3* and *Ccl9* promoters under any of the differentiation states tested, our 3C data demonstrated that the *Ccl4* and *Ccl5* promoters were in close proximity in both naive CD8⁺ T cells and effector CTLs (Figure S5). Taken together, these data suggest that extended chromatin looping of regulatory elements onto the *Ccl5* promoter is evident within naive CD8⁺ T cells.

Evidence of Transcriptional Co-regulation of *Ccl4* and *Ccl5*

The data presented earlier suggested that a physical interaction is evident between the *Ccl4* and *Ccl5* promoters. Therefore, we hypothesized that, within individual effector CTLs, we might observe co-regulation of both *Ccl5* and *Ccl4* transcription. To test this hypothesis, we performed single-cell RT-PCR to detect *Ccl4* and *Ccl5* transcripts in single, fluorescence-activated cell sorting (FACS)-purified IAV-specific CD8⁺ effector cells (>98% purity) (Figure 6A). As a positive control in these experiments, only cells in which we could detect β -actin (*ActB*) were included in our analysis (Figure 6A). Consistent with our hypothesis, we observed both *Ccl4* and *Ccl5* transcripts in ~44% of cells assayed (35 of 80 cells), with ~48% of cells exhibiting only *Ccl4* transcripts, and only 1 cell had only *Ccl5* transcript detectable in the absence of detectable *Ccl4* transcripts (Figure 6B). Thus, it appears that, as well as being co-transcriptionally linked to *Ccl5* transcription, *Ccl4* transcription precedes and, potentially, may be a prerequisite, for *Ccl5* transcription.

Figure 4. GATA3 Binding Is Enriched at H3K4me3⁺ TEs Linked to CD8⁺ Effector Gene Loci

GATA3 ChIP-seq was carried out on sort-purified naive or effector OT-I cells as described for Figure 1.

(A) Shown is the number of GATA3 peaks that were called for naive (red), effector (green), or both naive and effector (overlap) CD8⁺ OT-I T cells, with examples of associated gene loci.

(B) GATA3 binding overlaps with regulated H3K4me1/me2 TEs. Shown are ChIP-seq tracks for H3K4me1, me2, me3, and GATA3 in naive (blue) and effector (red) CD8⁺ OT-I T cells at CD8⁺ T cell gene loci.

(C) GATA3 binding is enriched at H3K4me3⁺ TEs in effector versus naive CD8⁺ OT-I cells.

(D) GATA3 binding at H3K4me3⁺ TEs is associated with greater transcription in naive (blue) versus effector (red) CD8⁺ OT-I T cells. RNA-seq data are from Russ et al. (2014).

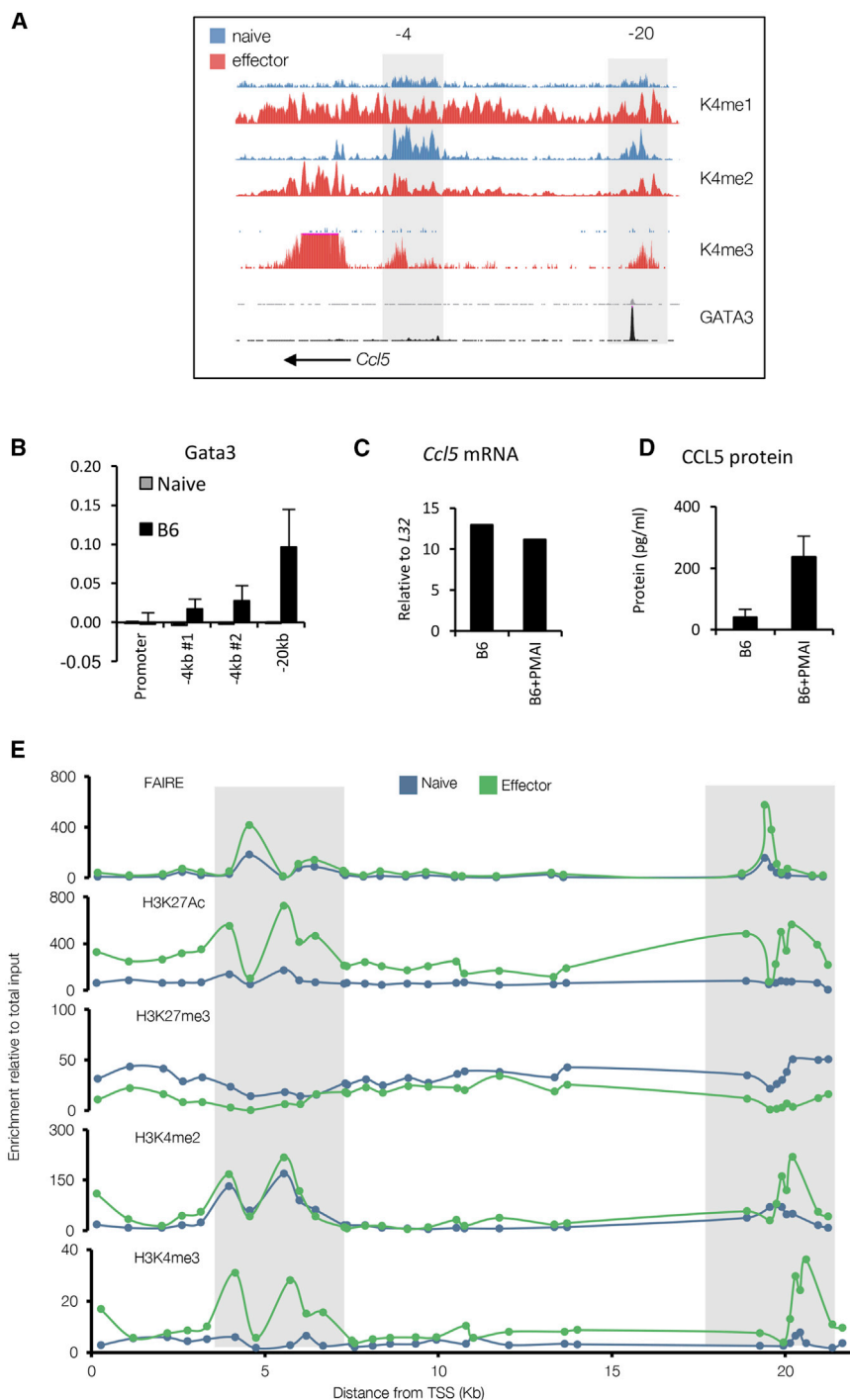


Figure 5. GATA3 Binding to H3K4me3⁺ TEs within the *Ccl5* Locus Is Associated with Permissive Histone PTMs in Effector OT-Is

(A) ChIP-seq tracks for H3K4me1, H3K4me2, H3K4me3, and GATA3 binding within the *Ccl5* locus in naive (blue) or effector (red) CD8⁺ OT-Is. (B) GATA3 ChIP was done on naive (CD44^{lo} CD62L^{hi}) or effector CD8⁺ OT-Is as described for Figure 1. Data indicate mean ± SEM from 3 independent experiments.

(C and D) Naive (CD44^{lo} CD62L^{hi}) CD8⁺ OT-1 T cells were sort purified *in vitro* and activated with 10 μg/mL plate-bound anti-CD3ε and anti-CD8α, and 5 μg/mL anti-CD11α in the presence of 10 U/mL recombinant human interleukin 2 (rhIL-2) and 5 μg/mL anti-CD28 antibody (Ab). Cells were harvested at 5 days and restimulated with phorbol 12-myristate 13-acetate (PMA)/ionomycin for 5 hr. (C) RNA was extracted from resting or stimulated cells, and cDNA was generated and used as a template for qPCR using L32 and *Ccl5* probes. (D) CCL5 protein expression was analyzed using cytokine bead array. Data indicate mean ± SEM from 3 independent experiments. (*p < 0.05 using unpaired Student's t test).

(E) ChIP analysis of the *Ccl5* locus after *in vitro* activation. Sort purified naive OT-1s were activated *in vitro* for 5 days. Cells were harvested at day 5 post-stimulation, fixed, and sonicated, and samples were subjected to FAIRE or ChIP analysis with antibodies directed against H3K27Ac, H3K27me3, H3K4me2, and H3K4me3. Samples were analyzed by real-time PCR using primer sets spanning the *Ccl5* TSS up to the putative -20-kb TE. The enrichment was normalized by total histone H3 ChIP (data not shown). Data shown are representative of 3 independent experiments. Highlighted are the putative -4-kb and -20-kb TEs identified via the ChIP-seq analysis (gray boxes) in either naive (blue lines) or effector (green lines) CD8⁺ OT-1 T cells.

changes in TE histone signatures are associated with the acquisition and maintenance of lineage-specific effector functions. Such dynamics included the acquisition or loss of H3K4me1⁺/me2⁺ in genomic regions unique to either the naive state or the E/M state; identification of poised enhancers (H3K4me1⁺/H3K4me2⁺/H3K27me3⁺) in naive CD8⁺ T cells that become active (H3K4me1⁺/H3K4me2⁺/H3K27Ac⁺) upon E/M differentiation; and, finally, identification of a

subset of active enhancers that gained H3K4me3 upon E/M differentiation.

Deposition of H3K4me2 at gene promoters within human hematopoietic stem cells transcriptionally poises developmentally important genes, thus enabling rapid cell-fate commitment (Orford et al., 2008). More recently, a similar pattern of H3K4me2 deposition has been reported to mark

DISCUSSION

The engagement of appropriate gene expression programs upon cellular differentiation is a critical feature of adaptive cellular immunity, yet how lineage-specific transcriptional programs arise and are maintained is not well understood. Here, we show that, during virus-specific CD8⁺ T cell differentiation, dynamic

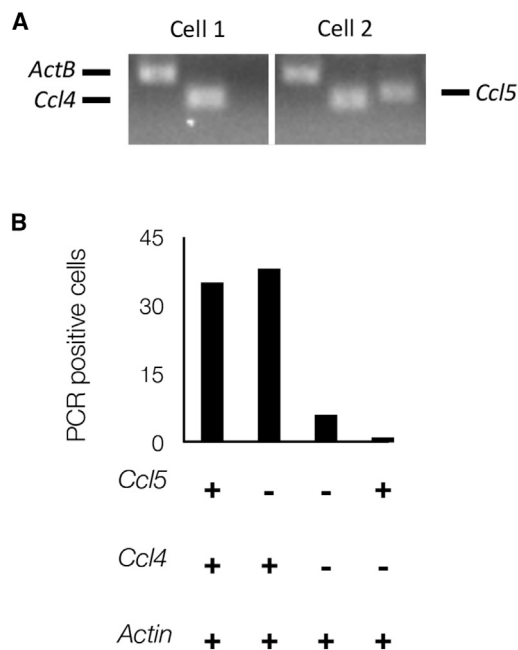


Figure 6. Single-Cell RT-PCR for *Ccl5* and *Ccl4* Co-transcription within Effector CD8⁺ T Cells

(A) Naive (CD44^{lo} CD62L^{hi}) CD8⁺ OT-I T cells were sort purified and *in vitro* activated as described in Figure 5. Cells were harvested and single-cell sorted into a well of a 96-well plate for cDNA synthesis as described previously (Turner et al., 2003). Nested RT-PCR was performed using primers specific for *Actb*, *Ccl4*, or *Ccl5* transcripts.

(B) Shown are the number of actin⁺ single cell, *in vitro* OT-I T cells that are also transcribed *Ccl4*, *Ccl5*, or both.

developmentally poised enhancer elements within developing thymocytes (Zhang et al., 2012). In this case, discrete peaks of H3K4me2 were associated with the CD3 genes (CD3 ϵ , $-\delta$, and $-\gamma$) within early CD4 CD8 double negative (DN) thymocyte 1 T cell precursors. Importantly, these loci also exhibited deposition of H3K27me3, indicating a poised enhancer chromatin signature. Subsequent maturation of DN1 into DN3/CD4 CD8 double positive (DP) thymocyte was associated with a deposition of H3K4me2, loss of H3K27me3, and stage-specific transcriptional upregulation of the CD3 genes. Similarly, we identified a significant number of discrete H3K4me1⁺/me2⁺ peaks that were linked to immune-related genes within the mature naive CD8⁺ T cell compartment that also exhibited a poised enhancer chromatin signature (H3K4me1⁺ H3K4me2⁺ H3K27me3⁺). Indeed, these findings support our earlier suggestion that, rather than H3K27me3 deposition acting as an epigenetic silencer, it acts as a molecular handbrake at key immune-related genes, both limiting their inappropriate transcription within naive cells and enabling their upregulation upon infection. This appears to be a mechanism at both gene promoters and TEs. Hence, the establishment of effective CTL responses involves coordinate chromatin remodeling at both promoter and non-coding regulatory elements (Denton et al., 2011; Nguyen et al., 2016; Russ et al., 2014; Araki et al., 2008, 2009; Northrop et al., 2008). It will be of further interest to determine the specific enzymes and TFs that regu-

late genome-wide changes in chromatin structure during virus-specific CD8⁺ T cell differentiation.

The specific combination of histone PTMs located within a given non-coding regulatory element can predict the specific role that particular TEs play in regulating cellular differentiation (Bulger and Groudine, 2011). For example, our data identified poised enhancers that acquired an active chromatin signature and that were linked to immune-related gene loci. An aspect of our data was the identification of a subset of the poised TEs that became active (H3K4me1⁺/me2⁺/H3K27Ac⁺) upon E/M CTL differentiation and also gained H3K4me3⁺—a modification typically associated with transcriptionally active promoter regions (Barski et al., 2007). Given the reported association of H3K4me3 in stabilizing the transcriptional potential of both enhancers and promoters in human CD4⁺ T cells (Chen et al., 2015), it is tempting to speculate that those loci where K4me3 deposition is acquired at unique TEs upon activation ensures transcriptional stability at gene loci associated with E/M CD8⁺ T cell function. The fact that the majority of H3K4me3⁺ enhancers were initially poised in the naive state suggests that this may be a mechanism that contributes to rapid and lineage-specific gene transcription upon the activation of naive CD8⁺ T cells. Importantly, our TFBS enrichment and TF ChIP-seq analysis demonstrated that the H3K4me3⁺ TEs are likely targets of TFs known to be essential regulators of virus-specific T cell differentiation, such as BATF/Jun, T-BET, RUNX3, GATA3, and PRDM1 (Cruz-Guilloty et al., 2009; Kallies et al., 2009; Wang et al., 2013; Xin et al., 2016). Thus, it is likely that K4me3⁺ TEs comprise a subset of regulatory regions that are key determinants for CTL differentiation. Determination of the functional significance of K4me3 deposition at TEs will be the focus of future studies.

Within the *Ccl5* and *Gzmb* gene loci of naive CD8⁺ T cells, we identified poised TEs (−5 kb and −20 kb for *Ccl5*; −23 kb for *Gzmb*) that became activated, with evidence of H3K4me3 deposition and GATA3 binding, upon differentiation. GATA3 has previously been reported to be key for sustaining virus-specific T cell proliferation (Wang et al., 2013). We have previously shown that GATA3 binding to the *Gzma* locus is associated with the deposition of transcriptionally permissive histone PTMs and *Gzma* transcription (Nguyen et al., 2016). Our data suggest that a mechanism by which GATA3 acts to support T cell differentiation might be via binding to and activation of TEs key for regulating T cell lineage-specific loci.

Finally, 3C analysis demonstrated that both the *Ccl5* −20-kb TE and *Ccl4* promoter, located 140 kb distant, were in close proximity to the *Ccl5* gene promoter in both naive and effector CD8⁺ T cells. Recent studies suggest that the regulated formation of promoter-promoter interactions allows coordinated expression of genes with similar functions (Chepelev et al., 2012). Of interest was the fact that *Ccl5* transcription was preceded by *Ccl4* transcription; hence, the *Ccl4* promoter may, in fact, be acting as a TE by helping “prime” transcriptional activation of the *Ccl5* gene. The establishment of a preconfigured higher order chromatin structure at the *Ccl5* locus is reminiscent of the ordered chromatin structures observed for the *Il4*, *Il5*, and *Il13* locus in naive CD4⁺ T cells that ensures

co-ordinate transcription of multiple gene loci (Spilianakis and Flavell, 2004). It has recently been determined that preconfiguration of chromatin structures is important for enabling cellular differentiation (Rubin et al., 2017). Given that we identified that *Ccl5* regulatory elements were pre-configured in naive CD8⁺ T cells to be in close proximity to the *Ccl5* promoter, and that they exhibited a “poised” TE signature that became active upon maturation, this suggests that perhaps naive CD8⁺ T cells are preconfigured for terminal differentiation upon activation. This provides a potential molecular explanation for earlier observations demonstrating that naive T cell activation results in a program of differentiation that can be largely antigen independent (Kaech and Ahmed, 2001; van Stipdonk et al., 2003). It remains to be determined whether such structures are observed at other signature CD8⁺ T cell gene loci, and whether these are truly unique to naive CD8⁺ T cells or are a reflection of general baseline interactions across many cell types. Future studies are aimed at determining whether this is, in fact, the case.

EXPERIMENTAL PROCEDURES

Mice, Viruses, and Infection

Ly5.2+ C57BL/6J (B6) and congenic Ly5.1+ OT-I mice were bred and housed under specific-pathogen-free conditions at either the Peter Doherty Institute for Infection and Immunity animal facility at the University of Melbourne or the Animal Resource Laboratory at Monash University. For infection, mice were anesthetized and infected i.n. with 10⁴ plaque-forming units (PFUs) of recombinant A/HKx31 virus engineered to express the OVA_{257–264} peptide (HKx31-OVA) in the neuraminidase stalk (Jenkins et al., 2006). All experiments were conducted according to approval obtained from the institutional animal ethics committee.

Adoptive Transfer, Tissue Sampling, Cell Culture, and CBA Analysis

For adoptive transfers, 10³ OT-I cells pooled from lymph nodes were injected intravenously (i.v.) 24 hr prior to infection with x31-OVA. For sorting effector and memory cells (10 and >60 days post-infection, respectively), lymphocyte preparations (10⁷/mL) were resuspended in PBS/0.1% fetal calf serum (FCS) and stained with anti-CD8a-FITC (fluorescein isothiocyanate) and anti-CD45.1-allophycocyanin (to detect OT-I cells). Naive cells (CD44^{lo}CD8⁺) were stained with CD44-FITC and CD8-allophycocyanin (APC). Cells were sorted using the BD FACSAria sorter (BD Biosciences). Samples were then analyzed with the BD FACSCanto (BD Biosciences, Nth Ryde, Australia) and FlowJo software (Ashland, OR, USA). Effector CTL cultures were seeded with 3.3 × 10⁵ sort-purified, naive (CD44^{lo}, CD62L^{hi}) CD8⁺ T cells. Cells were cultured in RPMI, supplemented with 10% FCS (v/v), 2 mM L-glutamine, and penicillin and streptomycin. Cultures were initiated in 6-well plates before being transferred to T75 flasks at day 2. Cultures were split 1:2 at day 4. Type 1 cultures were stimulated with plate-bound anti-CD3a (10 μg/mL), anti-CD8a (10 μg/mL), anti-CD28 (5 μg/mL), and anti-CD11a (10 μg/mL) antibodies and cultured in the presence of interleukin (IL)-2 (10 U/mL). Type 2 cultures were further supplemented with IL-4 (25 ng/mL) and anti-IFNG antibody (2 μg/mL). CBA assays were performed using the BD Biosciences Cytometric Bead Array Mouse Flex kit.

RNA Extraction, Real-Time PCR, and Single-Cell PCR

After sorting (naive cells) or following cell culture, RNA extractions were performed on ~5 × 10⁵ cells using TRIzol (Invitrogen) according to the manufacturer’s instructions. Reverse transcription was performed on 200–500 ng RNA using the Omniscript RT Kit (QIAGEN) according to the manufacturer’s instructions. ~25 ng equivalent of RNA was assayed using TaqMan Gene MGB primer/probe sets (Life Technologies). Data analysis was performed using the 2^{−ΔΔCt} method (Livak and Schmittgen, 2001). Single-cell PCRs were performed as described previously (Jenkins et al., 2007; Turner et al., 2003). Briefly, single cells

were sorted into 96-well plates, and reverse transcription was performed using the SuperScript VILO kit (Life Technologies, Mulgrave, Australia) according to the manufacturer’s instructions, with synthesis primed with oligo(dT) primers. Next, a first round of PCR amplification was performed using pooled external primers for *Ccl4*, *Ccl5*, and *ActB*. This first reaction was then split and used as a template for a second round of amplification, where internal primers for only a single gene product were used per reaction. Table S1 lists the primers used that were designed using the Primer3 program (Untergasser et al., 2012).

FAIRE, ChIP, and 3C Assays

ChIP was performed as described previously (Juelich et al., 2009; Russ et al., 2014). For histone PTMs, cells were fixed with 0.6% formaldehyde (final concentration) and, for GATA3, 6% formaldehyde. For FAIRE assays, cells were fixed with 0.6% formaldehyde, and following sonication, DNA was extracted twice with phenol:chloroform:isoamyl alcohol (25:24:1, v/v) before being precipitated with ethanol. The primers used for ChIP are described in Table S1. 3C was performed and analyzed as described previously (Hagège et al., 2007), using 1.5–2 × 10⁷ cells per assay. Briefly, cells were fixed with 1.5% formaldehyde (final) at room temperature (RT) for 10 min, and chromatin was digested with 400 U BglII (New England Biolabs, Ipswich, MA, USA) overnight (O/N) at 37°C, followed by the addition of a further 200 U and incubation for 2 hr. Primers and probes used are described in Table S1.

ChIP

ChIP was performed as previously described (Juelich et al., 2009; Russ et al., 2014) with the monoclonal antibodies to precipitate histones marked with H3K4me1, H3K4me2, H3K4me3 (clone 04-745, EMD Millipore, Bellerica, MA, USA), H3K27Ac, and H3K27me3 (clone Ab4729, Abcam, Cambridge, UK). After validating the specificity of each precipitation by real-time PCR via primers targeting characterized loci (Denton et al., 2011) (primers are described in Table S1), DNA fragments of 200 bp were purified from 10 ng of template and ligated to Illumina oligonucleotide adapters. Samples were then sequenced with an Illumina GAII or Hi-Seq 2000 sequencer and mapped to the mouse genome (build mm10) with the Bowtie software (Langmead and Salzberg, 2012). Analysis of the ChIP-seq data was performed as described previously (Russ et al., 2014). The H3K4me3 ChIP-seq for naive and effector OTI CTLs was done in duplicate. Analysis of ChIP-seq and TFBS enrichment is described in the Supplemental Information. The accession number for ChIP-seq and RNA-seq data reported in this paper is GEO: SRP049743 (Russ et al., 2014).

Statistical Analysis

Statistical analyses were performed using Prism GraphPad software. Error bars indicate SEM, and n values signify biological replicates.

SUPPLEMENTAL INFORMATION

Supplemental Information includes Supplemental Experimental Procedures, five figures, and four tables and can be found with this article online at <https://doi.org/10.1016/j.celrep.2017.11.097>.

ACKNOWLEDGMENTS

The authors would like to thank Drs. Nicole La Gruta and Colby Zaph for discussion and helpful suggestions. We would also like to acknowledge the support of the Micromon Sequencing platform at Monash University for NGS services. This work was supported by grants from the National Health and Medical Research Council of Australia (program grant #5671222 awarded to S.J.T. and project grant #APP1003131 awarded to S.J.T. and S.R.). S.J.T. is supported by an NHMRC Principal Research Fellowship.

AUTHOR CONTRIBUTIONS

Conceptualization, S.J.T., B.E.R., and S.R.; Methodology, B.E.R., J.L., M.L.T.N., L.J.G., and M.O.; Formal Analysis, M.O. and L.J.G.; Investigation,

B.E.R., M.L.T.N., M.R.O., H.A.M., S.N., T.H.O.N., and G.K.; Resources, D.J.F.P. and P.J.H.; Writing – Original Draft, S.J.T. and B.E.R.; Writing – Review & Editing, B.E.R., J.L., L.J.G., S.R., S.J.T.; Supervision, S.R. and S.J.T.; Funding Acquisition, S.R. and S.J.T.

DECLARATION OF INTERESTS

The authors declare no competing interests.

Received: October 31, 2016

Revised: August 8, 2017

Accepted: November 28, 2017

Published: December 19, 2017

REFERENCES

- Agarwal, S., and Rao, A. (1998). Modulation of chromatin structure regulates cytokine gene expression during T cell differentiation. *Immunity* 9, 765–775.
- Araki, Y., Fann, M., Wersto, R., and Weng, N.P. (2008). Histone acetylation facilitates rapid and robust memory CD8 T cell response through differential expression of effector molecules (eomesodermin and its targets: perforin and granzyme B). *J. Immunol.* 180, 8102–8108.
- Araki, Y., Wang, Z., Zang, C., Wood, W.H., 3rd, Schones, D., Cui, K., Roh, T.Y., Lhotsky, B., Wersto, R.P., Peng, W., et al. (2009). Genome-wide analysis of histone methylation reveals chromatin state-based regulation of gene transcription and function of memory CD8+ T cells. *Immunity* 30, 912–925.
- Balasubramani, A., Shibata, Y., Crawford, G.E., Baldwin, A.S., Hatton, R.D., and Weaver, C.T. (2010). Modular utilization of distal cis-regulatory elements controls *Irfng* gene expression in T cells activated by distinct stimuli. *Immunity* 33, 35–47.
- Balasubramani, A., Winstead, C.J., Turner, H., Janowski, K.M., Harbour, S.N., Shibata, Y., Crawford, G.E., Hatton, R.D., and Weaver, C.T. (2014). Deletion of a conserved *cis*-element in the *Irfng* locus highlights the role of acute histone acetylation in modulating inducible gene transcription. *PLoS Genet.* 10, e1003969.
- Barski, A., Cuddapah, S., Cui, K., Roh, T.Y., Schones, D.E., Wang, Z., Wei, G., Chepelev, I., and Zhao, K. (2007). High-resolution profiling of histone methylations in the human genome. *Cell* 129, 823–837.
- Bauer, W.R., Hayes, J.J., White, J.H., and Wolffe, A.P. (1994). Nucleosome structural changes due to acetylation. *J. Mol. Biol.* 236, 685–690.
- Bulger, M., and Groudine, M. (2011). Functional and mechanistic diversity of distal transcription enhancers. *Cell* 144, 327–339.
- Chen, K., Chen, Z., Wu, D., Zhang, L., Lin, X., Su, J., Rodriguez, B., Xi, Y., Xia, Z., Chen, X., et al. (2015). Broad H3K4me3 is associated with increased transcription elongation and enhancer activity at tumor-suppressor genes. *Nat. Genet.* 47, 1149–1157.
- Chepelev, I., Wei, G., Wangsa, D., Tang, Q., and Zhao, K. (2012). Characterization of genome-wide enhancer-promoter interactions reveals co-expression of interacting genes and modes of higher order chromatin organization. *Cell Res.* 22, 490–503.
- Cruz-Guilloty, F., Pipkin, M.E., Djuretic, I.M., Levanon, D., Lotem, J., Lichtenheld, M.G., Groner, Y., and Rao, A. (2009). Runx3 and T-box proteins cooperate to establish the transcriptional program of effector CTLs. *J. Exp. Med.* 206, 51–59.
- Denton, A.E., Russ, B.E., Doherty, P.C., Rao, S., and Turner, S.J. (2011). Differentiation-dependent functional and epigenetic landscapes for cytokine genes in virus-specific CD8+ T cells. *Proc. Natl. Acad. Sci. USA* 108, 15306–15311.
- Djuretic, I.M., Levanon, D., Negreanu, V., Groner, Y., Rao, A., and Ansel, K.M. (2007). Transcription factors T-bet and Runx3 cooperate to activate *Irfng* and silence *Ii4* in T helper type 1 cells. *Nat. Immunol.* 8, 145–153.
- Giresi, P.G., Kim, J., Daniell, R.M., Iyer, V.R., and Lieb, J.D. (2007). FAIRE (Formaldehyde-Assisted Isolation of Regulatory Elements) isolates active regulatory elements from human chromatin. *Genome Res.* 17, 877–885.
- Hagège, H., Klous, P., Braem, C., Splinter, E., Dekker, J., Cathala, G., de Laat, W., and Forné, T. (2007). Quantitative analysis of chromosome conformation capture assays (3C-qPCR). *Nat. Protoc.* 2, 1722–1733.
- Jenkins, M.R., Webby, R., Doherty, P.C., and Turner, S.J. (2006). Addition of a prominent epitope affects influenza A virus-specific CD8+ T cell immunodominance hierarchies when antigen is limiting. *J. Immunol.* 177, 2917–2925.
- Jenkins, M.R., Kedzierska, K., Doherty, P.C., and Turner, S.J. (2007). Heterogeneity of effector phenotype for acute phase and memory influenza A virus-specific CTL. *J. Immunol.* 179, 64–70.
- Juelich, T., Sutcliffe, E.L., Denton, A., He, Y., Doherty, P.C., Parish, C.R., Turner, S.J., Tremethick, D.J., and Rao, S. (2009). Interplay between chromatin remodeling and epigenetic changes during lineage-specific commitment to granzyme B expression. *J. Immunol.* 183, 7063–7072.
- Kaech, S.M., and Ahmed, R. (2001). Memory CD8+ T cell differentiation: initial antigen encounter triggers a developmental program in naïve cells. *Nat. Immunol.* 2, 415–422.
- Kallies, A., Xin, A., Belz, G.T., and Nutt, S.L. (2009). Blimp-1 transcription factor is required for the differentiation of effector CD8(+) T cells and memory responses. *Immunity* 31, 283–295.
- Kouzarides, T. (2007). Chromatin modifications and their function. *Cell* 128, 693–705.
- Kurachi, M., Barnitz, R.A., Yosef, N., Odorizzi, P.M., Dilorio, M.A., Lemieux, M.E., Yates, K., Godec, J., Klatt, M.G., Regev, A., et al. (2014). The transcription factor BATF operates as an essential differentiation checkpoint in early effector CD8+ T cells. *Nat. Immunol.* 15, 373–383.
- Langmead, B., and Salzberg, S.L. (2012). Fast gapped-read alignment with Bowtie 2. *Nat. Methods* 9, 357–359.
- Livak, K.J., and Schmittgen, T.D. (2001). Analysis of relative gene expression data using real-time quantitative PCR and the 2^{-ΔΔCT} method. *Methods* 25, 402–408.
- McLean, C.Y., Bristor, D., Hiller, M., Clarke, S.L., Schaar, B.T., Lowe, C.B., Wenger, A.M., and Bejerano, G. (2010). GREAT improves functional interpretation of cis-regulatory regions. *Nat. Biotechnol.* 28, 495–501.
- Muralidharan, S., Hanley, P.J., Liu, E., Chakraborty, R., Bollard, C., Shpall, E., Rooney, C., Savoldo, B., Rodgers, J., and Dotti, G. (2011). Activation of Wnt signaling arrests effector differentiation in human peripheral and cord blood-derived T lymphocytes. *J. Immunol.* 187, 5221–5232.
- Nguyen, M.L., Hatton, L., Li, J., Olshansky, M., Kelso, A., Russ, B.E., and Turner, S.J. (2016). Dynamic regulation of permissive histone modifications and GATA3 binding underpin acquisition of granzyme A expression by virus-specific CD8(+) T cells. *Eur. J. Immunol.* 46, 307–318.
- Northrop, J.K., Wells, A.D., and Shen, H. (2008). Cutting edge: chromatin remodeling as a molecular basis for the enhanced functionality of memory CD8 T cells. *J. Immunol.* 181, 865–868.
- Olson, M.R., Russ, B.E., Doherty, P.C., and Turner, S.J. (2010). The role of epigenetics in the acquisition and maintenance of effector function in virus-specific CD8 T cells. *IUBMB Life* 62, 519–526.
- Orford, K., Kharchenko, P., Lai, W., Dao, M.C., Worhunsky, D.J., Ferro, A., Janzen, V., Park, P.J., and Scadden, D.T. (2008). Differential H3K4 methylation identifies developmentally poised hematopoietic genes. *Dev. Cell* 14, 798–809.
- Pearce, E.L., Poffenberger, M.C., Chang, C.H., and Jones, R.G. (2013). Fueling immunity: insights into metabolism and lymphocyte function. *Science* 342, 1242454.
- Pekowska, A., Benoukraf, T., Zacarias-Cabeza, J., Belhocine, M., Koch, F., Holota, H., Imbert, J., Andrau, J.C., Ferrier, P., and Spicuglia, S. (2011). H3K4 tri-methylation provides an epigenetic signature of active enhancers. *EMBO J* 30, 4198–4210.
- Rubin, A.J., Barajas, B.C., Furlan-Magaril, M., Lopez-Pajares, V., Mumbach, M.R., Howard, I., Kim, D.S., Boxer, L.D., Cairns, J., Spivakov, M., et al. (2017). Lineage-specific dynamic and pre-established enhancer-promoter contacts cooperate in terminal differentiation. *Nat. Genet.* 49, 1522–1528.

- Russ, B.E., Olshansky, M., Smallwood, H.S., Li, J., Denton, A.E., Prier, J.E., Stock, A.T., Croom, H.A., Cullen, J.G., Nguyen, M.L., et al. (2014). Distinct epigenetic signatures delineate transcriptional programs during virus-specific CD8(+) T cell differentiation. *Immunity* *41*, 853–865.
- Schoenborn, J.R., Dorschner, M.O., Sekimata, M., Santer, D.M., Shnyreva, M., Fitzpatrick, D.R., Stamatoyannopoulos, J.A., and Wilson, C.B. (2007). Comprehensive epigenetic profiling identifies multiple distal regulatory elements directing transcription of the gene encoding interferon-gamma. *Nat. Immunol.* *8*, 732–742.
- Spilianakis, C.G., and Flavell, R.A. (2004). Long-range intrachromosomal interactions in the T helper type 2 cytokine locus. *Nat. Immunol.* *5*, 1017–1027.
- Spitz, F., and Furlong, E.E. (2012). Transcription factors: from enhancer binding to developmental control. *Nat. Rev. Genet.* *13*, 613–626.
- Turner, S.J., Diaz, G., Cross, R., and Doherty, P.C. (2003). Analysis of clonotype distribution and persistence for an influenza virus-specific CD8+ T cell response. *Immunity* *18*, 549–559.
- Untergasser, A., Cutcutache, I., Koressaar, T., Ye, J., Faircloth, B.C., Remm, M., and Rozen, S.G. (2012). Primer3—new capabilities and interfaces. *Nucleic Acids Res.* *40*, e115.
- van Stipdonk, M.J., Hardenberg, G., Bijker, M.S., Lemmens, E.E., Droin, N.M., Green, D.R., and Schoenberger, S.P. (2003). Dynamic programming of CD8+ T lymphocyte responses. *Nat. Immunol.* *4*, 361–365.
- Veiga-Fernandes, H., Walter, U., Bourgeois, C., McLean, A., and Rocha, B. (2000). Response of naïve and memory CD8+ T cells to antigen stimulation in vivo. *Nat. Immunol.* *1*, 47–53.
- Visel, A., Blow, M.J., Li, Z., Zhang, T., Akiyama, J.A., Holt, A., Plajzer-Frick, I., Shoukry, M., Wright, C., Chen, F., et al. (2009). ChIP-seq accurately predicts tissue-specific activity of enhancers. *Nature* *457*, 854–858.
- Wang, Z., Zang, C., Rosenfeld, J.A., Schones, D.E., Barski, A., Cuddapah, S., Cui, K., Roh, T.Y., Peng, W., Zhang, M.Q., and Zhao, K. (2008). Combinatorial patterns of histone acetylations and methylations in the human genome. *Nat. Genet.* *40*, 897–903.
- Wang, Y., Misumi, I., Gu, A.D., Curtis, T.A., Su, L., Whitmire, J.K., and Wan, Y.Y. (2013). GATA-3 controls the maintenance and proliferation of T cells downstream of TCR and cytokine signaling. *Nat. Immunol.* *14*, 714–722.
- Xin, A., Masson, F., Liao, Y., Preston, S., Guan, T., Gloury, R., Olshansky, M., Lin, J.X., Li, P., Speed, T.P., et al. (2016). A molecular threshold for effector CD8(+) T cell differentiation controlled by transcription factors Blimp-1 and T-bet. *Nat. Immunol.* *17*, 422–432.
- Zhang, J.A., Mortazavi, A., Williams, B.A., Wold, B.J., and Rothenberg, E.V. (2012). Dynamic transformations of genome-wide epigenetic marking and transcriptional control establish T cell identity. *Cell* *149*, 467–482.
- Zhu, J., Yamane, H., and Paul, W.E. (2010). Differentiation of effector CD4 T cell populations (*). *Annu. Rev. Immunol.* *28*, 445–489.